Inhibition of Mammalian Target of Rapamycin by Rapamycin Causes the Regression of Carcinogen-Induced Skin Tumor Lesions

Panomwat Amornphimoltham, Kantima Leelahavanichkul, Alfredo Molinolo, Vyomesh Patel, and J. Silvio Gutkind

Abstract

Purpose: The activation of Akt/mammalian target of rapamycin (mTOR) pathway represents a frequent event in squamous cell carcinoma (SCC) progression, thus raising the possibility of using specific mTOR inhibitors for the treatment of SCC patients. In this regard, blockade of mTOR with rapamycin prevents the growth of human head and neck SCC cells when xenotransplanted into immunodeficient mice. However, therapeutic responses in xenograft tumors are not always predictive of clinical anticancer activity.

Experimental Design: As genetically defined and chemically induced animal cancer models often reflect better the complexity of the clinical setting, we used here a two-step chemical carcinogenesis model to explore the effectiveness of rapamycin for the treatment of skin SCC.

Results: Rapamycin exerted a remarkable anticancer activity in this chemically induced cancer model, decreasing the tumor burden of mice harboring early and advanced tumor lesions, and even recurrent skin SCCs. Immunohistochemical studies on tumor biopsies and clustering analysis revealed that rapamycin causes the rapid decrease in the phosphorylation status of mTOR targets followed by the apoptotic death of cancer cells and the reduction in the growth and metabolic activity of the surviving ones, concomitant with a decrease in the population of cancer cells expressing mutant p53. This approach enabled investigating the relationship among molecular changes caused by mTOR inhibition, thus helping identify relevant biomarkers for monitoring the effectiveness of mTOR inhibition in the clinical setting.

Conclusions: Together, these findings provide a strong rationale for the early evaluation of mTOR inhibitors as a molecular targeted approach to treat SCC.

Cancer arises in multistep process resulting from the sequential accumulation of genetic defects and the clonal expansion of selective cell populations (1). For example, in the case of human head and neck squamous carcinomas (HNSCC), tumor progression often involves the sequential genetic or epigenetic inactivation of multiple tumor suppressor genes, such as *p16* (9p21), *APC* (5q21-22), and *p53* (17p13; ref. 2), concomitant with changes in the activation state of signaling pathways that promote the aberrant growth of the cancerous cells. The latter frequently result from the overexpression and/or activity of cell surface receptors, including epidermal growth factor receptors, hepatocyte growth factor receptors (c-Met), and receptors for numerous cytokines, chemokines, and inflammatory mediators (3–5). These receptors share the ability to promote the

activation of several intracellular signaling pathways, including the Ras-mitogen-activated protein kinase kinase-extracellular signal-regulated kinase biochemical route and the phosphatidylinositol 3-kinase-Akt-mammalian target of rapamycin (mTOR) pathway, which in turn promote cell proliferation and survival (6). This emerging knowledge on the nature of the signaling networks driving the unrestricted growth of cancerous cells has now enabled the development of novel therapies targeting key signaling molecules whose dysregulation contribute to tumor progression in each cancer type.

In particular, the widespread activation of the phosphatidylinositol 3-kinase/Akt/mTOR pathway in HNSCC progression has raised the possibility of using specific mTOR inhibitors and their derivatives for the treatment of HNSCC patients (7, 8). In this regard, blockade of mTOR with rapamycin exerts a potent antitumoral effect and even prevents minimal residual disease in several human HNSCC xenograft models (9–11).

However, effectiveness in human xenograft tumors is not always predictive of a clinical anticancer activity (12, 13). Genetically defined and chemically induced animal cancer models are often more difficult to treat than xenotransplanted human tumors in immunocompromised mice but reflect better the more complex and challenging situation of the clinical setting (12–14). Thus, in this study, we took advantage of the well-established two-step chemical carcinogenesis model, in which squamous carcinogenesis (SCC) is initiated by the topical application of a tobacco-related chemical carcinogen

---

Translational Relevance

Activation of the Akt/mammalian target of rapamycin (mTOR) pathway frequently occurs in the progression of squamous cell carcinoma (SCC), making it possible to use specific mTOR inhibitors for SCC treatment. We show here that rapamycin exerts a potent anticancer activity in a well-established chemically induced skin cancer model, as chronic administration of rapamycin decreases the tumor burden in mice harboring early and advanced primary tumoral lesions, and even recurrent SCCs. Together with the potent antitumoral activity of rapamycin analogues (rapalogs) in numerous solid tumors, and the recent approval by the Food and Drug Administration of their use in advanced renal carcinoma, our present findings provide a strong rationale for the early evaluation of mTOR inhibitors as a molecular targeted approach to treat SCC. We have also identified here several biological relevant biomarkers that can be used to monitor the effectiveness of mTOR inhibitors in the clinical setting.

[7,12-dimethylbenz(a)anthracene (DMBA)] to the skin followed by the prolonged treatment with phorbol esters [12-O-tetradecanoylphorbol-13-acetate (TPA); ref. 15], to explore the effectiveness of rapamycin for the treatment of skin SCC lesions. We show here that rapamycin exerts a potent anticancer activity in this chemically induced cancer model, as chronic administration of rapamycin decreases the tumor burden of mice harboring early and advanced primary tumor lesions and even recurrent SCC. Indeed, the inhibition of mTOR with rapamycin results in the regression of carcinogen-induced skin SCC, thus providing a strong rationale for the early clinical evaluation of rapamycin and its derivatives in SCC patients.

Materials and Methods

Reagents. DMBA was purchased from Sigma and phorbol ester TPA was from Alexis Biochemicals. Rapamycin was provided by the Developmental Therapeutics Program (National Cancer Institute).

Antibodies. Polyclonal rabbit antibodies against phospho-Akt (pAkt; S473), phospho-S6 (pS6), eIF4E, and cyclin D1 were purchased from Cell Signaling. Rat monoclonal anti-mouse CD31 (BD Pharmingen), polyclonal rabbit anti-mouse CD3 (Dako), rat monoclonal anti-F4/80 (Serotec), rabbit polyclonal anti-p53 (Novocastra), rabbit polyclonal anti-glucose transporter 1 (Chemicon), polyclonal rabbit anti-vascular endothelial growth factor (Santa Cruz Biotechnology), and mouse monoclonal anti-proliferating cell nuclear antigen (PCNA; Zymed) were used when indicated.

Animals. All animal studies were carried out according to NIH-approved protocols, in compliance with the Guide for the Care and Use of Laboratory Animals. Six-week-old female FVB/N mice were obtained from Taconic Farm, Inc., housed in appropriate sterile filter-capped cages, and fed and watered *ad libitum*. All handling, tumor induction, and treatment procedures were conducted in a laminar flow biosafety hood.

Tumor induction and rapamycin treatment. Mice were shaved in the back and tumors were initiated by the topical treatment with a single dose of DMBA (100 μg/200 μL in acetone) followed by the tumor promotion phase in which mice were treated twice weekly with TPA (12.5 μg/200 μL in acetone) for 24 wk. The number and diameter of

each tumor was measured weekly. Rapamycin treatment was started when papillomas were first observed for the study of early lesion, approximately 9 to 10 wk after the initiation, or once the tumors achieved the indicated tumor burden for advanced lesions (16-18 wk). Drug administration of tumor-bearing animals was essentially done as previously described (7). Briefly, tumor-bearing animals were randomly divided into two groups and treated with rapamycin (10 mg/kg/d) or an equal volume of diluent (an aqueous solution of 5.2% Tween 80 and 5.2% polyethylene glycol). For early lesions, treatment schedule was a single injection per animal, per day, given i.p., for 5 consecutive days. For advanced and recurrent lesions, rapamycin was administered daily until the end of the study. Animals from each group were euthanized for tissue retrieval at the indicated time points. Tumor tissues were immediately collected after sacrificed and fixed in buffered zinc formalin (Z-fix, Anatech) at room temperature for 12 h. The tissues were then transferred to 70% alcohol and processed for paraffin embedding for histopathologic and immunohistochemical analysis.

Immunohistochemistry. The tissue slides were deparaffinized in xylene, hydrated through graded alcohols and distilled water, and rinsed with PBS. Antigen retrieval was done using a citrate buffer (pH 6) in a microwave for 20 min (2 min at 100% power and 18 min at 10% power). Slides were allowed to cool down for 30 min, rinsed twice with PBS, and incubated in 3% hydrogen peroxide in PBS for 10 min to quench the endogenous peroxidase. The sections were then washed in distilled water and PBS and incubated in blocking solution (2% bovine serum albumin in PBS-1% Tween 20) for 1 h at room temperature. Excess solution was discarded and the sections were incubated with the primary antibody diluted in blocking solution at 4°C overnight. After washing with PBS, the slides were sequentially incubated with the biotinylated secondary antibody (1:400; Vector Laboratories) for 30 min followed by the ABC complex (Vector Stain Elite, ABC kit, Vector Laboratories) for 30 min at room temperature. The slides were washed and developed in 3,3′-diaminobenzidine (Sigma FASTDAB tablet, Sigma Chemical) under microscopic observation. The reaction was stopped in tap water and the tissues were counterstained with Mayer's hematoxylin, dehydrated, and mounted. The images were taken using a Carl Zeiss Axioplan 2 microscope (Carl Zeiss, Inc. North America). The evaluation of the immunohistochemistry was conducted blindly, without knowledge of the origin and status of the treatment. The whole tissues were examined and classified based on the staining intensity (1, weak staining; 2, moderate staining; and 3, strong staining) and the percentage of positive cells (0, <10% of stained cells; 1, 10%-25%; 2, 25%-50%; 3, 50-75%; and 4, 75-100% of cells stained). Results were scored by multiplying the percentage of positive cells by the intensity (7, 16).

Immunofluorescence double staining. The OCT-embedded tissues were cut onto the silanated glass slides at 15 μm thickness with cryostat, air dried, and stored at -80°C. To process for immunofluorescence staining, the cryosections were thawed at room temperature, hydrated in distilled water, and washed thoroughly with PBS. The sections were then incubated in the blocking solution (5% heat-inactivated goat serum in 0.1% Triton X-100 PBS) for 1 h at room temperature. Excess solution was discarded and the sections were incubated with the first primary antibody diluted 1:100 in blocking solutions at 4°C overnight. After washing with PBS, the slides were sequentially incubated with the biotinylated secondary antibody (1:300; Vector Laboratories) for 1 h followed by the Texas red avidin antibody (Vector Stain Elite, ABC kit) for 30 min at room temperature. The slides were washed and incubated in avidin/biotin blocking kit (Vector Laboratories) for 15 min each followed by incubation in the blocking solution before repeating the staining process with the second primary antibody as described above. The fluorescein-labeled antibody against species of primary antibody was used as secondary antibody. The tissues were then mounted in Vectashield mounting medium with 4′,6-diamidino-2-phenylindole (DAPI; Vector Laboratories).

p53 mutation analysis. Tumors from vehicle- and rapamycin-treated mice (1-7 d of treatment) were subjected to mutation analysis of *p53*.
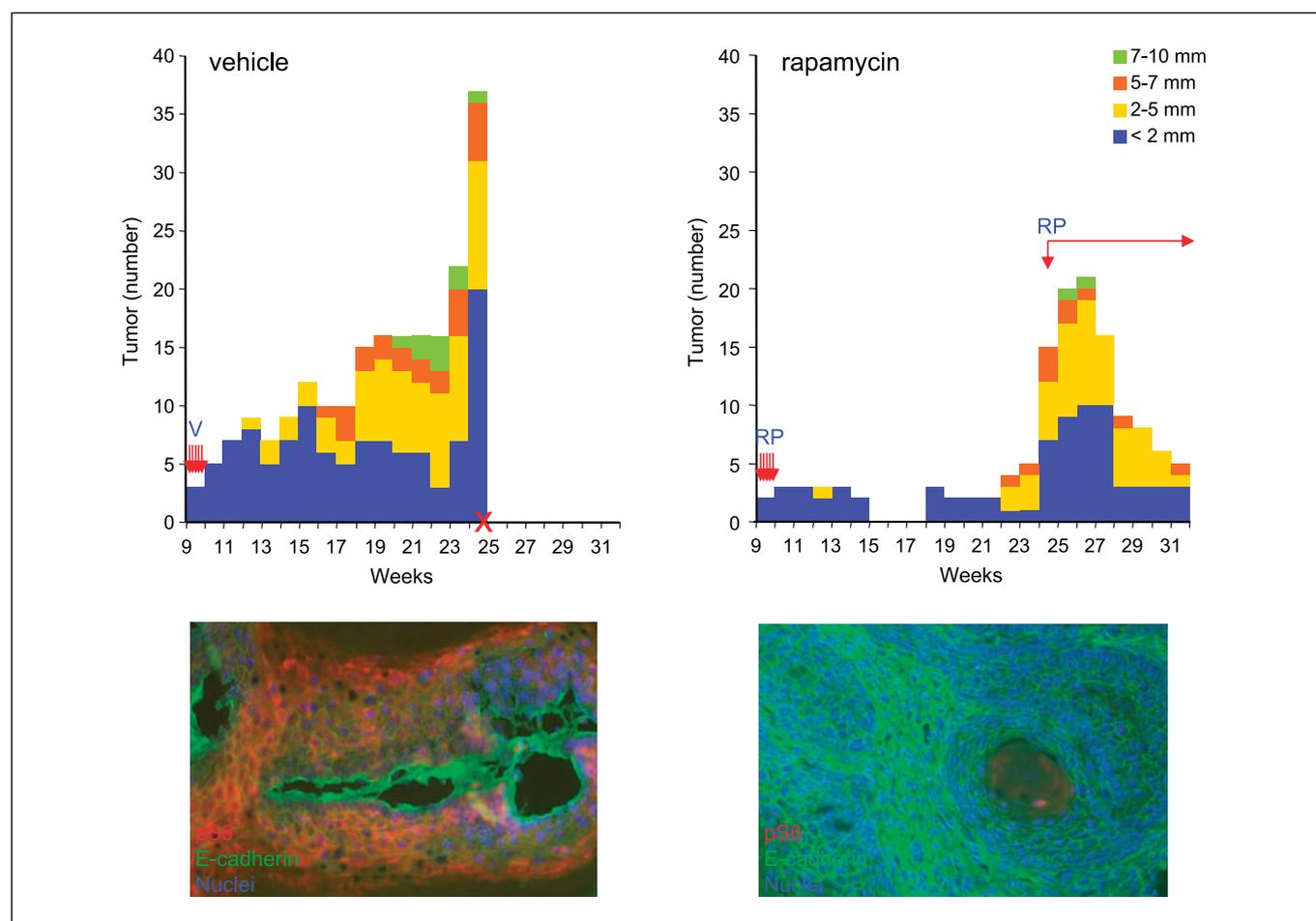
Fig. 1. Antitumoral effects of rapamycin in early lesions of chemically induced skin tumors. Mice were treated with a single dose of the carcinogen DMBA (initiation) followed by the twice weekly treatment with TPA (promotion). The number and diameter of each tumor was measured weekly and plotted as a function of time (weeks) after the exposure to DMBA. Rapamycin (*RP*; 10 mg/kg) or vehicle (*V*) treatment started at week 9. The second phase of the rapamycin treatment in the rapamycin-treated group was reinitiated at week 24, as indicated. Bar, number of tumors of each size (indicated by color coding). Arrows, rapamycin treatment. X, week in which mice had to be sacrificed due to their tumor burden. Representative immunofluorescence analysis of the tissues from the corresponding vehicle- and rapamycin-treated animals. The pS6 (*red*) immunodetection reflected the mTOR status and *E-cadherin* (*green*) was used to label tumor cells. Cell nuclei were stained with DAPI (*blue*).

Exons 4 to 9 of *p53* were amplified by PCR from genomic DNA (10-50 ng per reaction) with specific oligonucleotide primers. The primers used for PCR are as follows: exon 4, 5′-TAGGCTGAGAACACA-GTCCTGAGG-3′ (sense) and 5′-GCATTGAAAGGTCACACGAAAGAC-3′ (antisense); exon 5, 5′-CCTGATCGTTACTCGGCTTGTC-3′ (sense) and 5′-CAACTGTCTCTAAGACGCACAAACC-3′ (antisense); exon 7, 5′-TGTAGTGAGGTAGGGAGCGACTTC-3′ (sense) and 5′-GGGTAGGAAC-CAAAGAGCGTT-3′ (antisense); and exon 8+9, 5′-GCAGATATGACAA-GAGGGGTTG-3′ (sense) and 5′-GCGAGAGACAGAGGCAATAAGG-3′ (antisense). PCR products were sequenced directly in both directions with a 3730 DNA Analyzer (Applied Biosystems). Sequence traces were assembled and analyzed to identify potential genomic alterations using the Mutation Explorer software package (SoftGenetics) when compared with the sequence for all annotated exons and adjacent intronic sequences extracted from Reference assembly National Center for Biotechnology Information database (NT_096135.5).[1]

Terminal deoxynucleotidyl transferase–mediated dUTP nick end labeling assay. The tissue sections were dewaxed in xylene and rehydrated in graded ethanol and distilled water. After washing thrice with PBS, the slides were incubated with proteinase K (20 μg/mL in

PBS; Qiagen) for 20 min at room temperature, and the terminal deoxynucleotidyl transferase–mediated dUTP nick end labeling (TUNEL) staining was carried out using the *In situ* Cell Death Detection (Texas red kit; Boehringer Mannheim Biochemicals) according to the manufacturer's instructions. The tissues were then mounted in Vectashield mounting medium with DAPI.

Retro-orbital blood collection. The retro-orbital blood collection from medial canthus was done as described in NIH animal protocol and guideline. Briefly, a microhematocrit tube was inserted through the conjunctiva and into the orbital sinus by quickly rotating the tube. After the required amount of blood was obtained, the tube was withdrawn and blood was collected into collection tube (BD micro-tainer tubes with K_2EDTA; BD Biosciences) and bleeding ceases by the eye pressure.

Hierarchical clustering, data visualization, and statistical analysis. The staining scores that resulted from immunohistochemistry were converted into scaled values centered on zero (e.g., a score of 0 is converted to -2, 2 to 1, and 4 to 3) in Microsoft excel. The hierarchical analysis was done using Cluster program[2] with average linkage based on Pearson's correlation coefficient as the selection variable on the unsupervised approach. The results were visualized using the Java TreeView software. The clustered data were arranged with markers on the horizontal axis and tissue samples on the vertical axis as recently described (8). Two biomarkers with a close relationship are located next

---

[1]http://www.ncbi.nlm.nih.gov/
[2] http://rana.lbl.gov/EisenSoftware.htm

to each other. Unpaired t test was used to analyze the differences of tumor burden between experimental groups. Data analysis was done with GraphPad Prism version 4.00 for Windows (GraphPad Software); P values of <0.05 were considered statistically significant.

Results and Discussion

To investigate whether inhibition of mTOR by rapamycin may represent a suitable targeted therapy for skin tumor lesions, we began by inducing the formation of tumors in mice by the topical application of a single dose of a carcinogen, DMBA, followed by the chronic application of tumor promoter, TPA. When mice ($n = 10$) started developing skin tumoral lesions (9 weeks of TPA treatment; Fig. 1), they were divided into two groups and treated with rapamycin or vehicle for 5 consecutive days. This treatment proved to be effective in diminishing the accumulation of pS6 (Fig. 1, *bottom*), a direct downstream target of mTOR (17). The effect of rapamycin on the skin neoplasias was remarkable. Although the number and size of the tumors continued to increase in the control animals, this 5-day treatment with rapamycin was sufficient to decrease the tumor multiplicity and to induce complete tumor regression after 6 weeks (Fig. 1B).

All control mice had to be euthanized 25 weeks after starting the TPA treatment due to their weight loss (Fig. 1A). In the rapamycin-treated group, some tumors began recurring 10 weeks after completing the rapamycin administration (week 19 of the chemical carcinogenesis protocol; Fig. 1B). To assess the efficacy of rapamycin on these recurring tumor lesions, we initiated a second phase of rapamycin treatment at week 24 (tumors $n = 15$; 3.3 ± 0.3 mm) and extended the daily administration until the end of week 31 (tumors $n = 5$; 3.1 ± 0.7 mm). Even when these tumors had relapsed and were in a very advanced stage, rapamycin still reduced effectively their multiplicity ($P = 0.0001$).

These results prompted us to investigate the anticancer effects of the rapamycin in advanced stages of tumor progression (control group 10 mice, tumors $n = 21$, 3.1 ± 0.3 mm; treatment group 10 mice, tumors $n = 22$, 3.9 ± 0.4 mm; Fig. 2). The response to rapamycin treatment was evident by the reduction of the tumor burden as early as 1 week after initiating the treatment, observing a gradual regression of the tumors thereafter. Vehicle-treated animals had to be sacrificed at week 6 after the initiation of vehicle administration due to the overwhelming tumor burden (tumors $n = 68$, 3.8 ± 0.4 mm). A total of 22 representative tumors were collected for further analysis, 12 of which were diagnosed histopathologically as
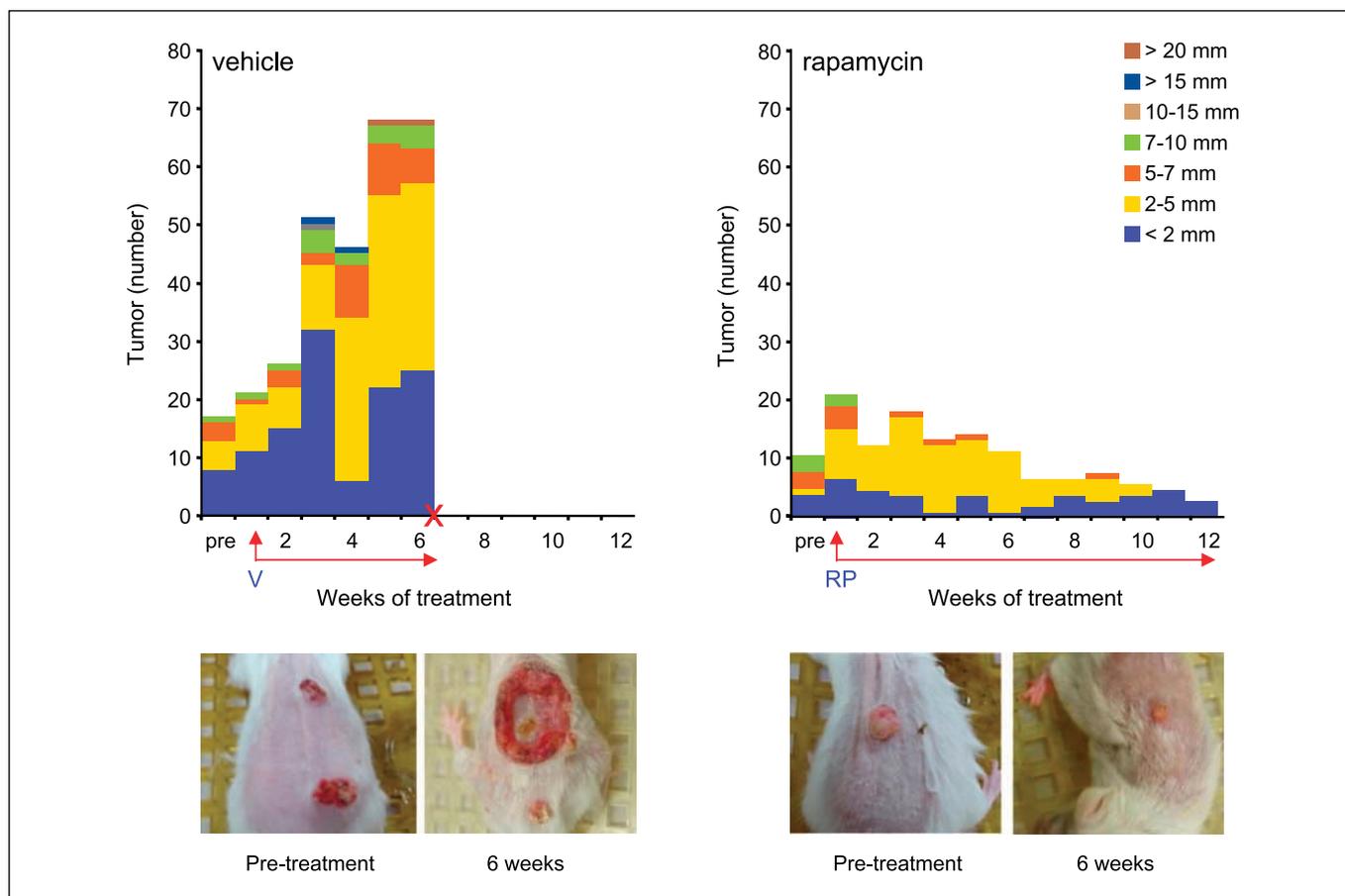

Fig. 2. Antitumoral effect of rapamycin in advanced skin cancer lesions. The number and size of chemically induced tumors in mice treated with vehicle and rapamycin (10 mg/kg) was depicted as for Fig. 1. Bar, number of tumors of the indicated size based on their designated color coding. Rapamycin treatment was initiated when most of the animals had at least one to two large tumors, as indicated. The control group had to be sacrificed 6 wk after treatment initiation with vehicle, as indicated with an X. Arrows, rapamycin or vehicle treatment. Representative tumors were photographed before rapamycin initiation (*Pre-treatment*) and after 6 wk of the initial treatment with rapamycin or vehicle control.

papillomas and 10 as SCC. At this particular time point, the rapamycin-treated group showed a significant lower tumor burden (tumors n = 13; 3.2 ± 0.2 mm, P < 0.0001; Fig. 2). Representative tumors from each group at week 6 of treatment are shown in Fig. 2. Only few small tumors were still visible at the end of the study, which was terminated after 12 weeks of rapamycin treatment (tumors n = 3, 2 ± 0 mm). All tumors were diagnosed as papillomas. These results indicate that rapamycin also exerts a potent antitumoral effect in advanced stages of chemically induced SCC.

Because rapamycin and its derivatives (rapalogs) act as immunosuppressive drugs (18), we explored whether the antitumor effect of rapamycin was related to this pharmacologic activity. Immunohistochemical analysis of animals treated in parallel with vehicle control or rapamycin for a prolonged time (6 weeks) revealed that there was no significant decrease in the number of macrophages, as recently reported (19), and T cells within the tumors and their surrounding tissues, suggesting that rapamycin does not affect the number of infiltrating inflammatory and immune cells in the tumor and stromal compartments (Table 1). Similarly, we did not see any significant reduction in the blood vessel density of these tumors, as judged by the use of anti-CD31 and anti-CD34 immunohistochemistry to detect tumor endothelial cells (Supplementary Fig. S1). On the other hand, analysis of blood samples from the animals exposed to rapamycin or vehicle for 6 weeks did not show any statistically significant difference in any of the blood cell components (Table 1). These data suggest that the antitumoral effects of rapamycin are not likely due to its antiangiogenic effect or a reduction in the overall number of circulating and tumor-infiltrating immune cells.

The effectiveness of rapamycin in diminishing the tumor burden in this chemically induced SCC model provided the opportunity to monitor and quantify the molecular signaling changes provoked by the treatment with rapamycin in a temporal manner. We focused on molecules related to the Akt/mTOR pathway (pS6, pAkt[Ser473], and eIF4E) and biomarkers reflecting the status of cell metabolism, cell proliferation, and cell death (p53, PCNA, cyclin D1, glucose transporter 1, and TUNEL assay) as well as tumor angiogenesis (vascular endothelial growth factor). A decrease in the level of pS6 in rapamycin-treated tumors clearly contrasts the high level of pS6 in the control group (Fig. 3A), reflecting the hyperactivity of the Akt/mTOR signaling pathway in SCC (9, 20). Concomitant with a reduction in pS6, we noted a decrease in cell proliferation, as judged by staining for PCNA and a cell cycle regulating cyclin, cyclin D1 (Fig. 3A).

One of the key genetic aberrations of chemically induced SCC mouse model is the presence of mutations in the *p53* tumor suppressor gene (15), which was nicely reflected by the high level of p53 expression by immunohistochemistry. The mutational status of the *p53* gene was confirmed by the sequence analysis of PCR-amplified genomic DNA from tumor samples from both control- and rapamycin-treated groups. Three of 10 tumors from the control group exhibited heterozygous mutation of p53 (245R>L, 55E>K, and 68A>E), which is aligned with prior studies using a similar chemical carcinogenesis approach (21). Sequencing of *p53* from the rapamycin-treated group revealed that three of seven tumors harbored heterozygous mutation of p53 (268E>Q, 239C>F, and 55E>K). Unexpectedly, however, we observed a reduction in the number of cells showing nuclear p53 in response to rapamycin treatment (Fig. 3A). This observation suggests that

Table 1. Complete blood count and immunohistochemical results from vehicle- and rapamycin-treated animals

Blood	Vehicle	Rapamycin
	Average (n = 7)	Average (n = 7)
WBC count (K/μL)	10.4 (4.7)	11.4 (4.7)
RBC count (M/μL)	6.3 (2.8)	7.2 (2.9)
Hemoglobin (g/dL)	11.3 (5.1)	12.7 (5.2)
Hematocrit (%)	33.7 (15.1)	35.1 (14.3)
MCV (fL)	57.4 (25.7)	49.9 (20.4)
Platelets (K/μL)	1,437.6 (642.9)	1,125.0 (459.3)
Polys (%)	44.7 (20.0)	37.1 (15.1)
Lymphocytes (%)	44.3 (19.8)	43.6 (17.8)
Monocytes (%)	8.7 (3.9)	15.9 (6.5)
Eosinophils (%)	0.9 (0.4)	0.5 (0.2)
Basophils (%)	1.6 (0.7)	3.0 (1.2)
Tumor tissues (immunohistochemistry)	**Vehicle**	**Rapamycin**
	Average* (n = 5)	Average* (n = 5)
T cells (CD3^{+})	96.4 (17.1)	97.6 (11.8)
Macrophage (F4/80^{+})	221.6 (10.5)	230.8 (41.2)

NOTE: Blood samples were collected from mice at advanced stages of tumor progression, as described in Fig. 2, after prolonged (6 wk) treatment with rapamycin and vehicle (see Materials and Methods). Standard complete blood cell components were analyzed. Immunohistochemistry for T cells markers (CD3^{+}) and macrophage markers (F4/80^{+}) was analyzed in tissue from the corresponding vehicle- and rapamycin-treated animals. Numbers are the mean (average) ± SE.
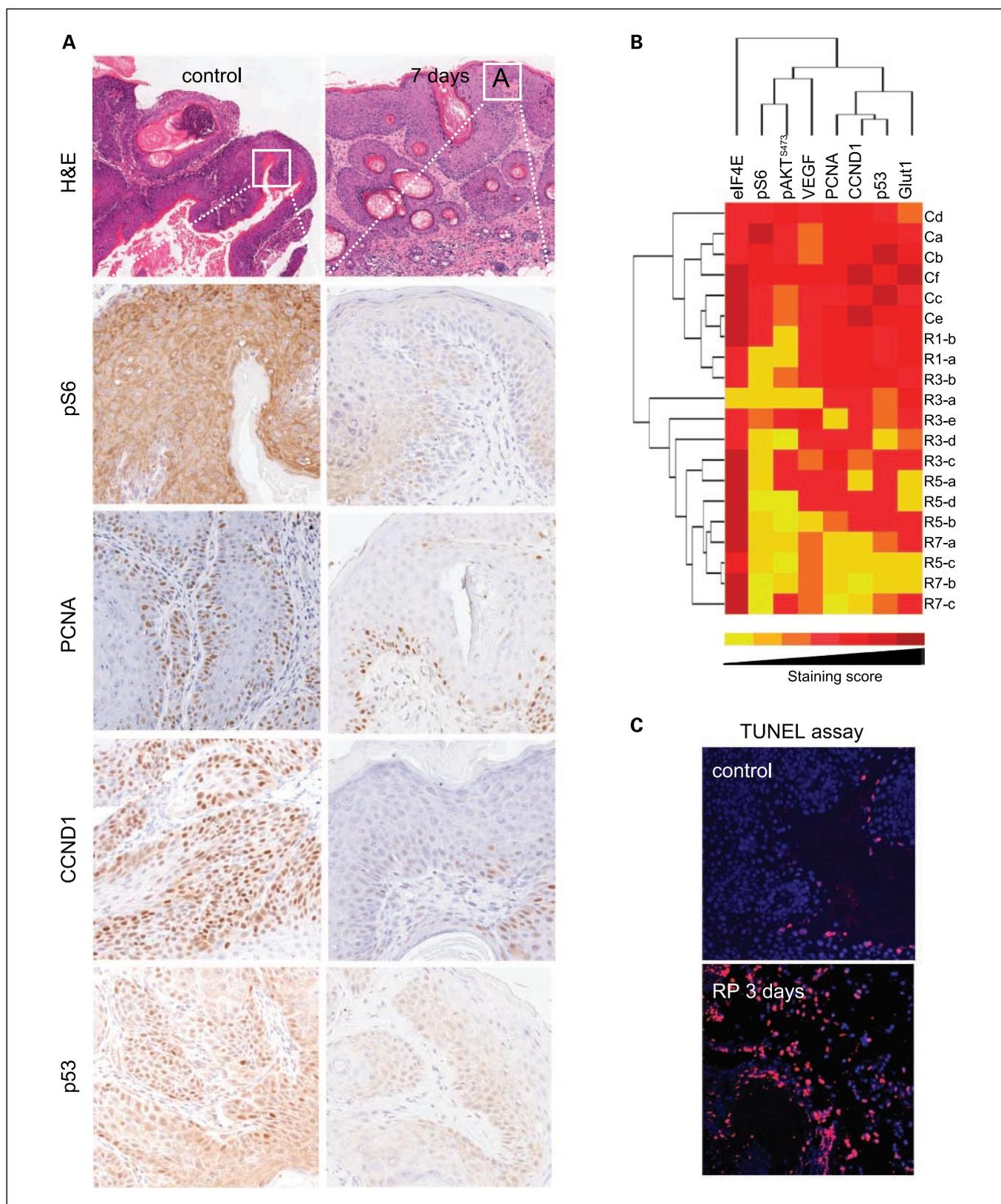Abbreviations: MCV, mean corpuscular volume; Polys, polymorphonuclear leukocytes.
*Arbitrary unit.

Fig. 3. Immunohistochemical analysis of biomarkers of rapamycin treatment response. *A,* immunohistochemistry from representative tumors acquired from control- and rapamycin-treated mice 7 d after initiating the rapamycin treatment as described in Fig. 2. The antibodies used are indicated. *B,* hierarchical clustering of immunohistochemical staining score against different biomarkers from the control tumors (*C*) and the papillomas harvested at different time points after rapamycin administration (*R1*, day 1; *R3*, day 3; *R5*, day 5; *R7*, day 7). Deep red, high staining scores (strong staining intensity and 75-100% of positive staining cells); yellow, low staining scores (weak staining intensity and <10% of cells positive for immunohistochemistry). *C,* TUNEL staining showing the apoptotic cells (*red*) of tumor sections from the control- and rapamycin-treated mice after 3 d of the rapamycin treatment initiation. Cell nuclei were stained with DAPI (*blue*).

few days of rapamycin treatment may not be sufficient to eliminate the tumor cell population bearing *p53* mutations but that these cells are sensitive to rapamycin, as previously reported (22), probably because mTOR inhibition may interfere with the expression of the mutant forms of p53 protein or may facilitate their degradation, an area that certainly warrants further investigation.

The nonsupervised hierarchical class comparison of the immunohistochemical data (8) revealed a strong temporal relationship among most of the samples in response to rapamycin treatment. For example, as shown in Fig. 3B, all control samples clustered together, and tissues collected after 1 day of treatment were adjacent to them. All samples collected after 3 days clustered together. All samples from animals treated for 5 and 7 days were closely clustered. From the heat map approach, it was clear that rapamycin began to be effective after 1 day of treatment and even more effective after 3 days, as judged by the decreased in pS6. This was partially reflected by a gradual decreased in the phosphorylation on Akt in S473, a target for the mTOR complex 2 (20). Indeed, pS6 and pAkt^{Ser473} clustered together in this analysis. This was only partially related to a smaller and slower decrease in the levels of vascular endothelial growth factor, which may explain the limited effect of rapamycin in tumor angiogenesis in these aggressive chemically induced tumors, in contrast to results obtained in xenograft models (9).

Of interest was also the observation that proliferative makers (cyclin D1 and PCNA) clustered together, in close relationship to p53, all of which began to be reduced with respect to controls after 5 to 7 days of treatment. The immunodetection of glucose transporter 1, which reflects an increased glucose metabolism (23), was more closely related to these molecules than to pS6, suggesting an interesting relationship between the metabolic state of the cells and their proliferative capacity. In contrast, the levels of eIF4E were not affected by the rapamycin treatment and served as an internal control. Similarly, whereas we have observed a rapid decrease in the levels of phosphorylated 4E-binding protein 1 (4E-BP1), a downstream target of mTOR that represses eIF4E-dependent translation (24), in HNSCC cells exposed to rapamycin (9), we did not observe a reproducible decrease of phosphorylated 4E-BP1 in chemically induced epithelial SCC on rapamycin treatment (data not shown). This observation raises the possibility that kinases other than mTOR may phosphorylate 4E-BP1 in SCC cells, including members of the mitogen-activated protein kinase and cyclin-dependent kinase superfamily, as previously reported (25–27), which may account for the rapamycin insensitivity of the phosphorylation of 4E-BP1. On the other hand, we also noticed that this clustering analysis divided the data into two separated groups at day 3 after rapamycin treatment (Fig. 3B). This is likely because in parallel with the antiproliferative effects of rapamycin, we also observed areas of massive apoptotic cell death on day 3 in the rapamycin-treated group, as revealed by

TUNEL labeling assays (Fig. 3C). Thus, rapamycin seems to cause the rapid inhibition of mTOR and a consequent reduction in pS6 and pAkt^{Ser473}. This is then followed by the apoptotic death of a fraction of the cancer cells and the reduction in the cell proliferation of the surviving ones, with a concomitant decrease in the population of cancer cells expressing high levels of mutant p53.

The increased molecular understanding of cancer has provided a wealth of opportunity for identifying novel therapies targeting molecular mechanisms that are dysregulated in particular cancer types. For example, in the case of SCC from the head and neck, recently available evidence indicates that activation of the Akt-mTOR signaling pathway is a widespread event, likely independently of the level of activation of epidermal growth factor receptor and the mutational status of p53 (8, 9). The use of mTOR inhibitors for the treatment of SCC could therefore represent a suitable approach. However, it is imperative to validate further the effectiveness of candidate drugs using animal models that reflect the complexity of the human disease better than classic xenograft models before pursuing their clinical evaluation in SCC patients. Indeed, although many differences between human cancers and chemically induced tumors in mice exist (12, 15), the classic two-stage chemical carcinogenesis model involving a tobacco carcinogen (DMBA) and the pro-proliferative effect of a tumor promoter (TPA) creates an environment permissive for cancer development leading to progressive squamous epithelial tumors that resemble human squamous cancers (28). In particular, using this model, we observed that rapamycin is effective in halting the tumor progression and causes the regression of both early papillomas and more advanced SCC, including those exhibiting mutant p53, thus reducing dramatically the tumor burden of tumor-bearing mice.

Together with the promising antitumoral activity of rapamycin and its analogues, CCI-779 and RAD001, in breast cancer, glioblastoma, and mantle cell lymphoma patients (18, 20), and the recent approval by the Food and Drug Administration of the use of CCI-779 (temsirolimus) in advanced renal carcinoma (29), our present findings provide a strong rationale for the early evaluation of mTOR inhibitors as a molecular targeted approach to treat SCC. Furthermore, the ability to investigate the relationship among molecular changes caused by mTOR inhibition by conventional immunohistochemistry may now provide several biological relevant biomarkers that can be used to monitor the effectiveness of mTOR inhibition in cancerous tissues in response to rapamycin and its analogues in the clinical setting.

Disclosure of Potential Conflicts of Interest

No potential conflicts of interest were disclosed.

References

1. Vogelstein B, Kinzler KW. Cancer genes and the pathways they control. Nat Med 2004;10:789–99.

2. Forastiere A, Koch W, Trotti A, Sidransky D. Head and neck cancer. N Engl J Med 2001;345:1890–900.

3. Patel V, Rosenfeldt HM, Lyons R, et al. Persistent activation of Rac1 in squamous carcinomas of the head and neck: evidence for an EGFR/Vav2 signaling axis involved in cell invasion. Carcinogenesis 2007;28:1145–52.

4. Pomerantz RG, Grandis JR. The role of epidermal growth factor receptor in head and neck squamous cell carcinoma. Curr Oncol Rep 2003;5:140–6.

5. Dorsam RT, Gutkind JS. G-protein-coupled receptors and cancer. Nat Rev Cancer 2007;7:79–94.

6. Shaw RJ, Cantley LC. Ras, PI(3)K and mTOR signalling

controls tumour cell growth. Nature 2006;441: 424 – 30.

7. Amornphimoltham P, Sriuranpong V, Patel V, et al. Persistent activation of the Akt pathway in head and neck squamous cell carcinoma: a potential target for UCN-01. Clin Cancer Res 2004;10:4029 – 37.

8. Molinolo AA, Hewitt SM, Amornphimoltham P, et al. Dissecting the Akt/mammalian target of rapamycin signaling network: emerging results from the head and neck cancer tissue array initiative. Clin Cancer Res 2007;13:4964 – 73.

9. Amornphimoltham P, Patel V, Sodhi A, et al. Mammalian target of rapamycin, a molecular target in squamous cell carcinomas of the head and neck. Cancer Res 2005;65:9953 – 61.

10. Nathan CO, Amirghahari N, Rong X, et al. Mammalian target of rapamycin inhibitors as possible adjuvant therapy for microscopic residual disease in head and neck squamous cell cancer. Cancer Res 2007;67: 2160 – 8.

11. Wislez M, Spencer ML, Izzo JG, et al. Inhibition of mammalian target of rapamycin reverses alveolar epithelial neoplasia induced by oncogenic K-ras. Cancer Res 2005;65:3226 – 35.

12. Frese KK, Tuveson DA. Maximizing mouse cancer models. Nat Rev Cancer 2007;7:645 – 58.

13. Lu SL, Herrington H, Wang XJ. Mouse models for human head and neck squamous cell carcinomas. Head Neck 2006;28:945 – 54.

14. Becher OJ, Holland EC. Genetically engineered models have advantages over xenografts for preclinical studies. Cancer Res 2006;66:3355 – 8, discussion 8 – 9.

15. DiGiovanni J. Multistage carcinogenesis in mouse skin. Pharmacol Ther 1992;54:63 – 128.

16. Charafe-Jauffret E, Tarpin C, Bardou VJ, et al. Immunophenotypic analysis of inflammatory breast cancers: identification of an 'inflammatory signature'. J Pathol 2004;202:265 – 73.

17. Affara NI, Trempus CS, Schanbacher BL, et al. Activation of Akt and mTOR in CD34+/K15+ keratinocyte stem cells and skin tumors during multi-stage mouse skin carcinogenesis. Anticancer Res 2006; 26:2805 – 20.

18. Vignot S, Faivre S, Aguirre D, Raymond E. mTOR-targeted therapy of cancer with rapamycin derivatives. Ann Oncol 2005;16:525 – 37.

19. Granville CA, Warfel N, Tsurutani J, et al. Identification of a highly effective rapamycin schedule that markedly reduces the size, multiplicity, and phenotypic progression of tobacco carcinogen-induced murine lung tumors. Clin Cancer Res 2007;13:2281 – 9.

20. Guertin DA, Sabatini DM. Defining the role of mTOR in cancer. Cancer Cell 2007;12:9 – 22.

21. Ruggeri B, Caamano J, Goodrow T, et al. Alterations of the p53 tumor suppressor gene during mouse skin tumor progression. Cancer Res 1991;51:6615 – 21.

22. Huang S, Liu LN, Hosoi H, Dilling MB, Shikata T, Houghton PJ. p53/p21 (CIP1) cooperate in enforcing rapamycin-induced G(1) arrest and determine the cellular response to rapamycin. Cancer Res 2001;61: 3373 – 81.

23. Gatenby RA, Gillies RJ. Why do cancers have high aerobic glycolysis? Nat Rev Cancer 2004;4:891 – 9.

24. Mamane Y, Petroulakis E, LeBacquer O, Sonenberg N. mTOR, translation initiation and cancer. Oncogene 2006;25:6416 – 22.

25. Mothe-Satney I, Brunn GJ, McMahon LP, Capaldo CT, Abraham RT, Lawrence JC Jr. Mammalian target of rapamycin-dependent phosphorylation of PHAS-I in four (S/T)P sites detected by phospho-specific antibodies. J Biol Chem 2000;275: 33836 – 43.

26. Wang X, Li W, Parra JL, Beugnet A, Proud CG. The C terminus of initiation factor 4E-binding protein 1 contains multiple regulatory features that influence its function and phosphorylation. Mol Cell Biol 2003; 23:1546 – 57.

27. Heesom KJ, Gampel A, Mellor H, Denton RM. Cell cycle-dependent phosphorylation of the translational repressor eIF-4E binding protein-1 (4E-BP1). Curr Biol 2001;11:1374 – 9.

28. Balmain A, Pragnell IB. Mouse skin carcinomas induced *in vivo* by chemical carcinogens have a transforming Harvey-ras oncogene. Nature 1983; 303:72 – 4.

29. Hudes G, Carducci M, Tomczak P, et al. Temsirolimus, interferon alfa, or both for advanced renal-cell carcinoma. N Engl J Med 2007;356: 2271 – 81.

Clinical Cancer Research

Inhibition of Mammalian Target of Rapamycin by Rapamycin Causes the Regression of Carcinogen-Induced Skin Tumor Lesions

Panomwat Amornphimoltham, Kantima Leelahavanichkul, Alfredo Molinolo, et al.

Updated version	Access the most recent version of this article at: http://clincancerres.aacrjournals.org/content/14/24/8094
Supplementary Material	Access the most recent supplemental material at: http://clincancerres.aacrjournals.org/content/suppl/2009/01/16/1078-0432.CCR-08-0703.DC1

Cited articles	This article cites 29 articles, 12 of which you can access for free at: http://clincancerres.aacrjournals.org/content/14/24/8094.full#ref-list-1
Citing articles	This article has been cited by 13 HighWire-hosted articles. Access the articles at: http://clincancerres.aacrjournals.org/content/14/24/8094.full#related-urls

E-mail alerts	Sign up to receive free email-alerts related to this article or journal.
Reprints and Subscriptions	To order reprints of this article or to subscribe to the journal, contact the AACR Publications Department at pubs@aacr.org.
Permissions	To request permission to re-use all or part of this article, use this link http://clincancerres.aacrjournals.org/content/14/24/8094. Click on "Request Permissions" which will take you to the Copyright Clearance Center's (CCC) Rightslink site.